

Investigation of the d(,n)p reaction for gamma beam monitoring at ELI-NP

To cite this article: C. Matei et al 2016 JINST 11 P05025

View the article online for updates and enhancements.

Related content

- Structure and Evolution of Single Stars: Hydrogen main sequence stars
 J MacDonald
- Experiments with brilliant gamma beams at ELI-NP: A glimpse in the future Dimiter L. Balabanski
- Brilliant gamma beams for industrial applications: new opportunities, new challenges

V Iancu, G Suliman, G V Turturica et al.

Recent citations

- Investigation of Compton scattering for gamma beam intensity measurements and perspectives at ELI-NP G.V. Turturica et al
- The extreme light infrastructure—nuclear physics (ELI-NP) facility: new horizons in physics with 10 PW ultra-intense lasers and 20 MeV brilliant gamma beams S Gales et al
- Brilliant gamma beams for industrial applications: new opportunities, new challenges
 V lancu et al



IOP ebooks™

Bringing you innovative digital publishing with leading voices to create your essential collection of books in STEM research.

Start exploring the collection - download the first chapter of every title for free.



RECEIVED: April 8, 2016 REVISED: May 12, 2016 ACCEPTED: May 22, 2016 PUBLISHED: May 31, 2016

Investigation of the $d(\gamma,n)p$ reaction for gamma beam monitoring at ELI-NP

C. Matei, a,1 J.M. Mueller, b,c M.H. Sikora, b,d G. Suliman, a C.A. Ur a and H.R. Weller, b,d

Horia Hulubei National Institute for R&D in Physics and Nuclear Engineering,

Bucharest-Magurele, 077125, Romania

Durham, North Carolina 27708, U.S.A.

 $^c Department\ of\ Nuclear\ Engineering,\ North\ Carolina\ State\ University,$

Raleigh, North Carolina 27695, U.S.A.

^dDepartment of Physics, Duke University,

Durham, North Carolina 27708, U.S.A.

E-mail: catalin.matei@eli-np.ro

ABSTRACT: The Extreme Light Infrastructure - Nuclear Physics facility will deliver brilliant gamma beams with high spectral density and a high degree of polarization starting in 2018 in Bucharest-Magurele, Romania. Several monitoring instruments are proposed for measuring the spectral, temporal, and spatial characteristics of the gamma beam. The $d(\gamma,n)$ p reaction has been investigated for its use in determining the gamma beam parameters in a series of measurements carried out at the High Intensity Gamma Source, Durham, U.S.A.. Measurements of the emitted neutrons have been performed using liquid scintillator and 6 Li-glass neutron detectors at several incident gamma energies between 2.5 to 20 MeV. The experimental results presented in this paper have shown that an instrument based on the $d(\gamma,n)$ p reaction can be used to monitor the intensity and polarization of the gamma beam to be produced at ELI-NP.

KEYWORDS: Beam-line instrumentation (beam position and profile monitors; beam-intensity monitors; bunch length monitors); Instrumentation and methods for time-of-flight (TOF) spectroscopy; Neutron detectors (cold, thermal, fast neutrons); Scintillators, scintillation and light emission processes (solid, gas and liquid scintillators)

^aExtreme Light Infrastructure — Nuclear Physics,

^bTriangle Universities Nuclear Laboratory,

¹Corresponding author.

C	Contents				
1	Introduction	1			
2	Method description	2			
	2.1 Photodisintegration of the deuteron	2			
	2.2 Beam polarization measurement	3			
	2.3 Beam intensity measurement	5			
3	Measurements at $HI\gamma S$ below $4 MeV$	6			
4	Measurements at $HI\gamma S$ above $4 MeV$	10			
5	Conclusion	14			

1 Introduction

The Extreme Light Infrastructure - Nuclear Physics (ELI-NP) facility in Romania consists of two major components: the High Power Laser System and the Gamma Beam System (GBS) [1]. ELI-NP will allow either combined or stand-alone experiments using the high-power lasers and the gamma beam.

The high brilliance Gamma Beam System at ELI-NP will deliver quasi-monochromatic gamma-ray beams (bandwidth better than 0.5%) with a high spectral density (higher than 10^4 photons/s/eV) and high degree of linear polarization (better than 99%). The GBS will be delivered in two phases with two separate beam lines: a low-energy gamma-ray line with gamma energies up to 3.5 MeV and a high-energy gamma-ray line with energies up to 19.5 MeV.

Optimization and monitoring of the gamma beam with these characteristics is challenging and requires the proper means for accurately measuring the spatial, spectral and temporal characteristics of the gamma-ray beams. The GBS will be equipped with a beam characterization station for each beam line which will be mainly used by the operators for the initial tuning of the gamma beam. Several additional gamma beam monitoring instruments are foreseen to be used for gamma beam monitoring and in conjunction with the proposed experimental stations.

The gamma beam energy spread will be monitored using a large volume HPGe detector with anti-Compton shield placed in the attenuated beam [2]. An intensity and polarization monitor is proposed based on the $d(\gamma,n)p$ reaction which could be placed in either the low-energy or the high-energy experimental areas. Several additional instruments using Compton scattering and photo-fission are envisioned for measuring the time structure, intensity, and polarization of the beam [2].

In this paper we present our investigation of the $d(\gamma,n)$ p reaction for intensity and polarization measurements of the gamma beam at ELI-NP. The organization of this paper is as follow: in

section 2 we review the state of the $d(\gamma,n)p$ cross section and polarization asymmetry data and their associated uncertainties. The method is detailed with the basic steps necessary for beam polarization and intensity calculations. Experimental tests at High Intensity Gamma Source (HI γ S) were carried out in November 2014 and July 2015 over a gamma-ray energy range from 2.5 to 20 MeV. Finally, based on these tests we conclude that the $d(\gamma,n)p$ reaction can be used for constructing an intensity and polarization instrument at ELI-NP.

2 Method description

2.1 Photodisintegration of the deuteron

The photodisintegration of the deuteron in the $d(\gamma,n)p$ reaction is a basic nuclear process which has been extensively studied for understanding the electromagnetic properties of the nucleons and the nucleon-nucleon interaction. Significant experimental and theoretical work has been invested into better measurements and calculations of the differential cross section and the polarization asymmetry. We restrict our review of the world data and theoretical calculations to the ELI-NP energy range of interest, i.e. from threshold to 20 MeV.

Experimental measurements of the $d(\gamma,n)p$ cross section started in the 1950's. These earlier results were of limited accuracy [3] and deviate from present measurements and theoretical calculations. Birenbaum et al. used in the 1980's an absorption method and (n,γ) reactions to obtain absolute cross sections with an accuracy of better than 3% in the energy range between 6 and 11.4 MeV [3]. Another result came in the same period from a monochromatic photon source at Frascati National Laboratories and a 4π proton detector [4]. The cross sections measured at two energies below 20 MeV, 14.7 and 19.3 MeV, were reported with 2% uncertainty [4].

Several reviews [5] of the world data have been published, mainly to check various theoretical models of the deuteron photodisintegration. Jaus et al. [5] used the Nijmegen 93 potential to calculate the total cross section and the some of these data are presented in tables 1 and 2. Tornow et al. [6] measured the photon analyzing power for the photodisintegration of the deuteron at several energies below 4 MeV and the data agreed very well with the theoretical prediction of Arenhovel et al. [7] presented in table 1 (also plotted in figure 1). It can be concluded from these comparisons that theoretical calculations based on different approaches give results which are in very good agreement with the experimental measurements. While there have been experimental measurements of the total cross section above 4 MeV, there is only one measurement at lower energies. The lack of total cross section measurements below 3.5 MeV should be addressed in the near future as these data are of primary importance for Big Bang Nucleosynthesis [8].

The threshold for photodisintegration of the deuteron is 2.23 MeV. The analyzing power goes to zero at threshold, but rises rapidly to 0.7 around 2.5 MeV and reaches 0.9 at 3.0 MeV. The maximum value is 0.97 at 6 MeV and it decreases slowly to 0.9 at 20 MeV. This means that this reaction can be used to measure the beam polarization at energies greater than 2.5 MeV. Top plot on left of figure 1 shows one calculation of the polarization asymmetry in the $d(\gamma,n)$ neutrons at a scattering angle of 90° [7].

We plotted in figure 1 the differential cross section at a scattering angle of 90° as calculated by Arenhovel et al. [7] using a potential model. This differential cross section is the same as

Table 1. Summary of the $d(\gamma,n)p$ experimental and theoretical polarization asymmetry, total, and differential cross section below 5 MeV photon energy. A_{pol} refers to the polarization asymmetry, the exp and th notations refer to experimental and theoretical, respectively.

E_{γ}	A_{pol}^{exp}	A_{pol}^{th} [7]	$\sigma_{exp}^{ m tot}$	$\sigma_{th}^{\mathrm{tot}}$ [7]	σ_{th}^{diff} [7]
(MeV)			(μb)	(μb)	(μb)
2.39	0.419(0.021)	0.437	-	839.1	7.89
2.48	0.649(0.019)	0.634	-	984.6	9.94
2.60	0.745(0.022)	0.760	-	1204.2	12.8
2.75	-	0.840	1456(45) [9]	1472.2	16.26
3.02	0.911(0.014)	0.903	-	1862.4	21.20
3.22	0.928(0.012)	0.922	-	2042.9	23.49
3.52	0.953(0.012)	0.944	-	2299.5	26.70
4.05	0.975(0.013)	0.959	-	2466.1	28.84

Table 2. Summary of the $d(\gamma,n)p$ polarization asymmetry, total, and differential cross section between 5 and 20 MeV photon energy.

E_{γ}	A th _{pol} [7]	$\sigma_{exp}^{ ext{tot}}$	$\sigma_{th}^{\rm tot}$ [5]	$\sigma_{th}^{\mathrm{tot}}$ [7]	σ_{th}^{diff} [7]
(MeV)	-	(μb)	(μb)	(μb)	$(\mu b $
5.97	0.972	2162(99) [3]	2228.6	2213.5	26.03
7.25	0.971	1882(11) [3]	1919.3	1913.5	22.49
7.60	0.970	1803(16) [3]	1841.4	1838.1	21.56
7.64	0.970	1810(28) [3]	1832.7	1828.0	21.48
8.80	0.967	1586(11) [3]	1601.7	1595.5	18.72
9.00	0.967	1570(36) [3]	1565.5	1558.4	18.27
11.39	0.956	1257(36) [3]	1205.4	1205.7	14.10
14.70	0.937	925(20) [4]	884.1	889.3	10.27
15.00	0.935	867(27) [10]	861.7	865.4	10.00
19.30	0.904	617(9) [4]	617.5	625.8	7.14
20.00	0.898	585(14) [<mark>10</mark>]	588.5	596.5	6.78

what would be expected when using an unpolarized or circularly polarized γ -ray beam. The cross section increases by a factor of two from 2.5 MeV to the maximum value of 2.9 mb at approximately 4.5 MeV. The cross section decreases to 0.68 mb at 20 MeV. Calculated and measured cross sections presented in table 2 are in very good agreement and the uncertainty on these data is below 5%.

2.2 Beam polarization measurement

Measurements at each energy have been performed using both circularly and linearly polarized beam. The measurement with 100% circularly polarized beam is used to correct for any instrumental asymmetries, such as differences in detector distances or detection efficiencies. Measurements with the linearly polarized beam are taken after the circularly polarized beam measurements. The

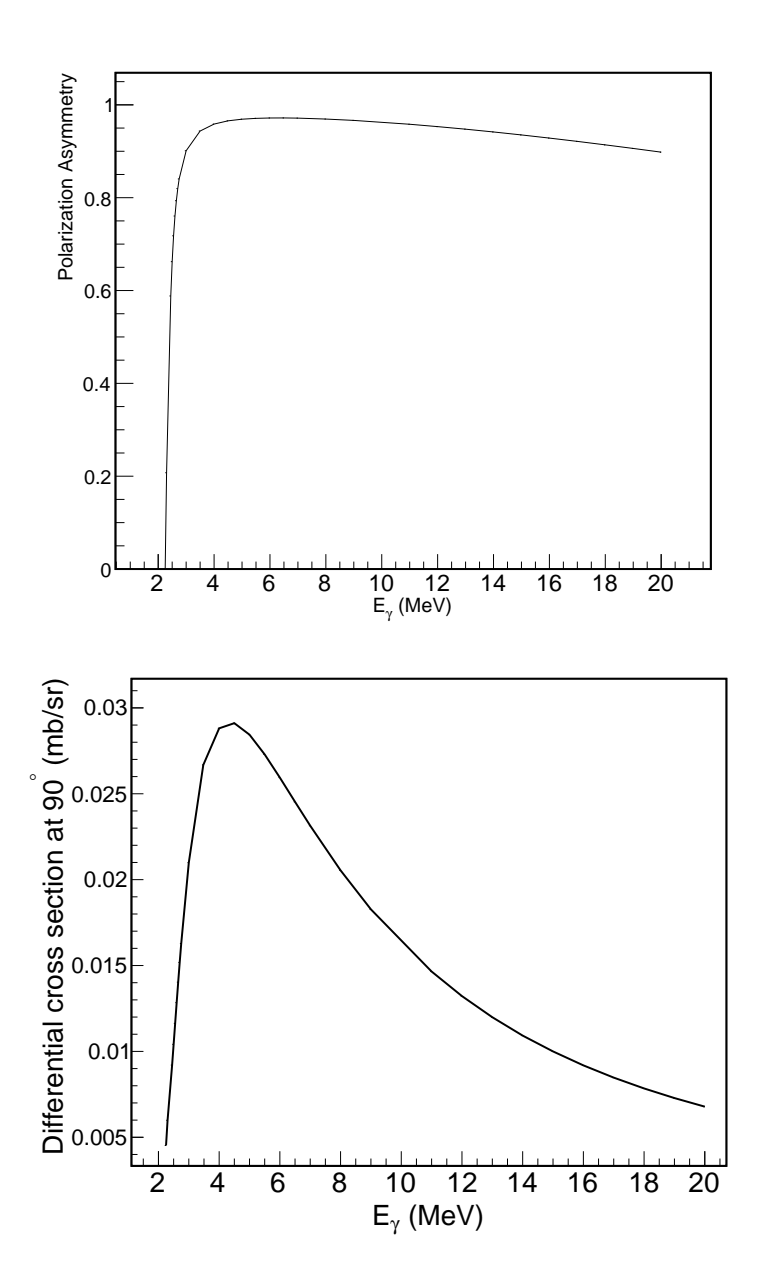


Figure 1. Theoretical calculation of the polarization asymmetry (top) and differential cross section (bottom) for outgoing neutrons scattered at 90° in the $d(\gamma,n)p$ reaction [7]

polarization asymmetry is defined by:

$$A_{\text{pol}} = \frac{\sum_{\text{in-plane}} \frac{Y^L}{Y^C} - \sum_{\text{out-plane}} \frac{Y^L}{Y^C}}{\sum_{\text{in-plane}} \frac{Y^L}{Y^C} + \sum_{\text{out-plane}} \frac{Y^L}{Y^C}},$$
(2.1)

where A_{pol} is the polarization asymmetry and $Y^{C,L}$ are the neutron yields after background subtraction measured by each detector with circularly and linearly polarized beams, respectively.

The beam polarization B_{pol} is determined from:

$$B_{\text{pol}} = \frac{A_{\text{pol}}^{\text{measured}}}{A_{\text{pol}}^{\text{expected}}},$$
(2.2)

where $A_{\rm pol}^{\rm measured}$ is the measured polarization asymmetry for a particular neutron energy cut and $A_{\rm pol}^{\rm expected}$ is the expected polarization asymmetry for that same neutron energy range. The expected polarization asymmetry is determined from folding the theoretical polarization asymmetries from ref. [7] with the beam energy distribution, target details, detector efficiencies, and the selected neutron energy range.

2.3 Beam intensity measurement

The photodisintegration of the deuteron could also be used to monitor the intensity of the beam by using a well-characterized neutron detection system. The beam intensity is inversely proportional to the differential cross section $d\sigma/d\Omega$:

$$\Phi = \frac{Y_{\text{in-plane}}}{\epsilon N_t \Delta \Omega} \left(\frac{d\sigma}{d\Omega} \right)^{-1} , \qquad (2.3)$$

where $Y_{\text{in-plane}}$ is the neutron yield of the in-plane neutron detector, ϵ is the neutron detection efficiency, N_t is the target thickness, and $\Delta\Omega$ is the solid angle covered by the detector.

The target thickness for a heavy water cell, N_t , can be calculated with the following equation [11]:

$$N_t = 2\frac{\rho N_A}{2M_d} + M_O L_{\text{cell}}, \qquad (2.4)$$

where N_A is the Avogadro's number, ρ is the density of heavy water, M_d and M_O are the mass of deuterium and oxygen, and L_{cell} is the length of the heavy water cell.

The neutron detectors used for the measurement of the gamma beam intensity should be carefully characterized. The first step of this procedure is to characterize Li-glass and NE213-type neutron detectors with gamma-rays for energy resolution and energy calibration of the pulse height axis. Experimental spectra are measured with calibrated gamma-ray sources (131 Sn, 22 Na, 137 Cs, and 65 Zn span a Compton energy range from 239 keV to 1061 keV). For NE213-type detectors, Monte Carlo codes such as MCNP or GRESP [12] are used to determine the theoretical Compton distributions for the gamma-ray lines used in the calibration procedure. The generated Compton spectrum is folded with a resolution function and fitted to the experimental detector response spectrum to determine the position of Compton edge. Energy calibration is necessary for setting reproducible threshold levels for the efficiency calculation.

The light output curve should also be constructed for NE213-type neutron detectors. This is important for comparing detectors made of different materials and also as an input function into Monte Carlo simulations. The light output curve is determined by measuring the detector response functions at various neutron energies. This procedure uses either mono-energetic neutrons or a 252 Cf time-tagged ionization chamber [13]. Standard neutron reference fields are available at National Metrological Institutes [14]: 144, 250, and 565 keV neutrons obtained with the 7 Li(p,n) 7 Be reaction are suitable for characterizing the 6 Li-glass detectors, while 1.25, 2.5 and 5 MeV neutrons obtained

with $T(p,n)^3$ He and $D(d,n)^3$ He are suitable for characterizing NE213-type detectors. The neutron detection efficiency is determined by comparing the experimental neutron energy spectrum to the Mannhart evaluation [15] when using the 252 Cf time-tagged ionization chambers or with the calculated neutron flux when using mono-energetic neutrons.

3 Measurements at HIγS below 4 MeV

Measurements have been carried out at $HI\gamma S$ in November 2014 and July 2015 at gamma energies between 2.5 and 3 MeV to test and optimize the method for monitoring the intensity and polarization described in section 2. The gamma-beam has been produced using the OK-4 method [16] which yields beams with linear polarization consistent with 100%.

The energy of the neutrons resulting from the $d(\gamma,n)p$ reaction is below 1 MeV for gamma-ray energies from threshold and up to 4 MeV. We used two ⁶Li-glass detectors as shown in figure 2 to measure the neutrons in this energy range. The detectors were placed at a scattering angle of 90° with one detector positioned in the plane of the beam polarization, detector designated as "beam-right detector", and the other positioned perpendicular to the plane of beam polarization (detector designated as "top detector"). Both detectors were approximately 15 cm from the center of the target.

The detectors manufactured by Saint-Gobain consisted of the 6 Li-glass, 5 cm in diameter and 0.95-cm thick, coupled by a quartz window to a Hamamatsu R-329 photomultiplier tube. Thin disks of copper, 2-mm thick, have been placed on the face of the detectors to reduce the gamma rays scattered from the target. The target consisted of heavy water (D_2O) encapsulated in a polyethylene container of 3.2 cm diameter and 5 cm length. The target container was suspended with a string system from the ceiling, thus reducing the amount of materials that could contribute to the scattered background. The beam was collimated using a 19 mm diameter lead collimator.

The detector signals were sent first to a fast bipolar amplifier (PS 771) to boost the gain from the PMTs. A beam pick-off monitor (BPO) located in the storage ring records the frequency of the produced γ -ray bursts. The BPO signal serves as the stop signal for the time-of-flight (TOF) measurements. The experiments carried out in November 2014 have used a conventional ADC and TDC to record the data, while in July 2015 the detector waveforms together with the BPO signal were read into a CAEN V1730 14-bit 500 Ms/s digitizer. We describe here the analysis of the data taken in July 2015 with the digitizer although the analysis procedure was identical for the previous runs.

The energy of the γ -ray beam was measured by placing a large HPGe detector in the attenuated beam. A Gaussian fit to the full energy peak revealed a gamma-beam energy of 2.997 MeV and a FWHM of 90 keV, corresponding to a beam spread of 3%.

The first measurement at each energy was performed using a 100% circularly polarized beam to correct for instrumental asymmetries. We then switched to 100% linearly polarized beams for the asymmetry measurement. Figure 3 shows the measured pulse height (PH) versus time-of-flight (TOF) spectra for the two detectors with a 100% linearly polarized gamma beam.

The peak below a TOF of 40 ns is the γ -flash. The γ -flash is originating from γ rays produced when the beam scatters off the target or other beam-line components. The peak is located around 33.5 ns for the out-of-plane detector and 36 ns for the in-plane detector. The FWHM of the gammaray peak in the TOF spectrum is 1.6 ns. The neutrons appear above 50 ns and at pulse heights above

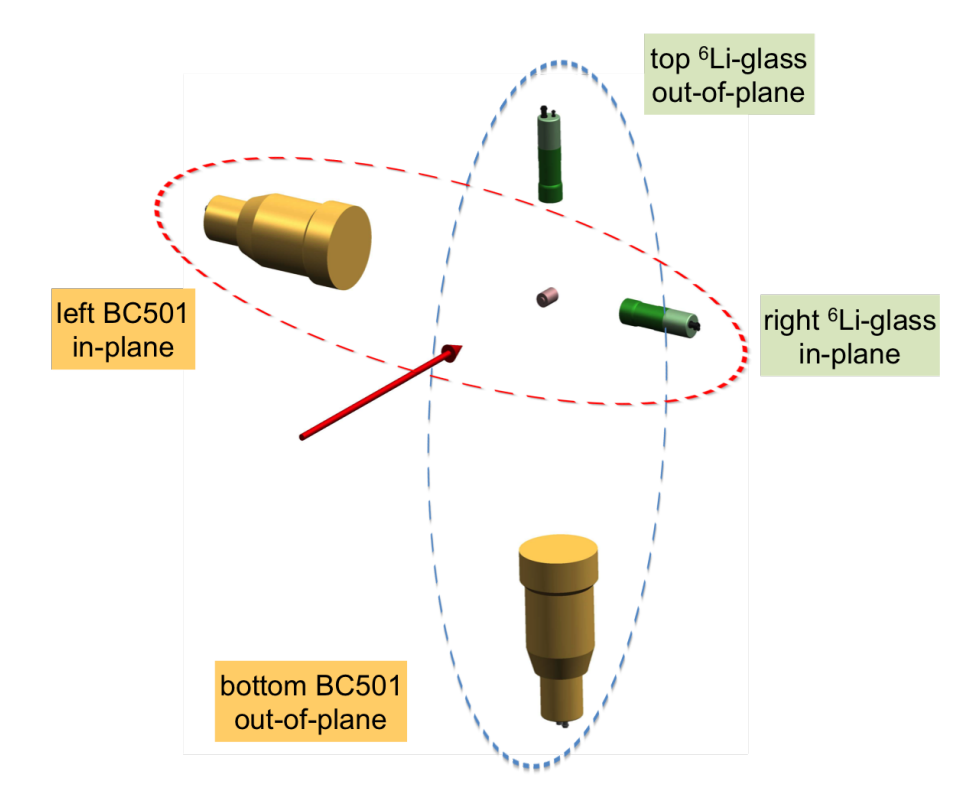


Figure 2. Diagram of the experimental configuration for the experiment in July 2015. The plane of the beam polarization is horizontal. The closest detectors are the two ⁶Li-glass detectors while the BC501 detectors are farther away.

30. There is very good separation between the gamma rays and neutrons from the PH vs TOF histogram in figure 3 which makes an additional cut on pulse height unnecessary.

The analysis of these data consisted in selecting a pulse height band which includes the neutron region from the PH vs. TOF spectrum and then plotting the time-of-flight spectrum. An example of time-of-flight spectrum for the in-plane and out-of-plane detectors with 100% linearly polarized beam is shown in figure 4. The arrow indicates the expected $384\,\text{keV}$ energy of the neutrons, corresponding to a TOF channel of 55.5 for the in-plane detector, for a mono-energetic beam of $2.997\,\text{MeV}$. The TOF spectrum of the out-of-plane detector has been shifted to align its γ -flash with the in-plane detector, although only the neutron part of the spectrum is shown in figure 4.

The 3% energy spread of the gamma beam, the TOF resolution, the extended target and detector mean that the neutrons impinging on the detector will cover a TOF range from 52 to 57 ns, corresponding to an energy range from 335 to 540 keV. The dashed lines indicate the summing window for determining the beam polarization. We preferred to do the analysis on the time-of-flight spec-

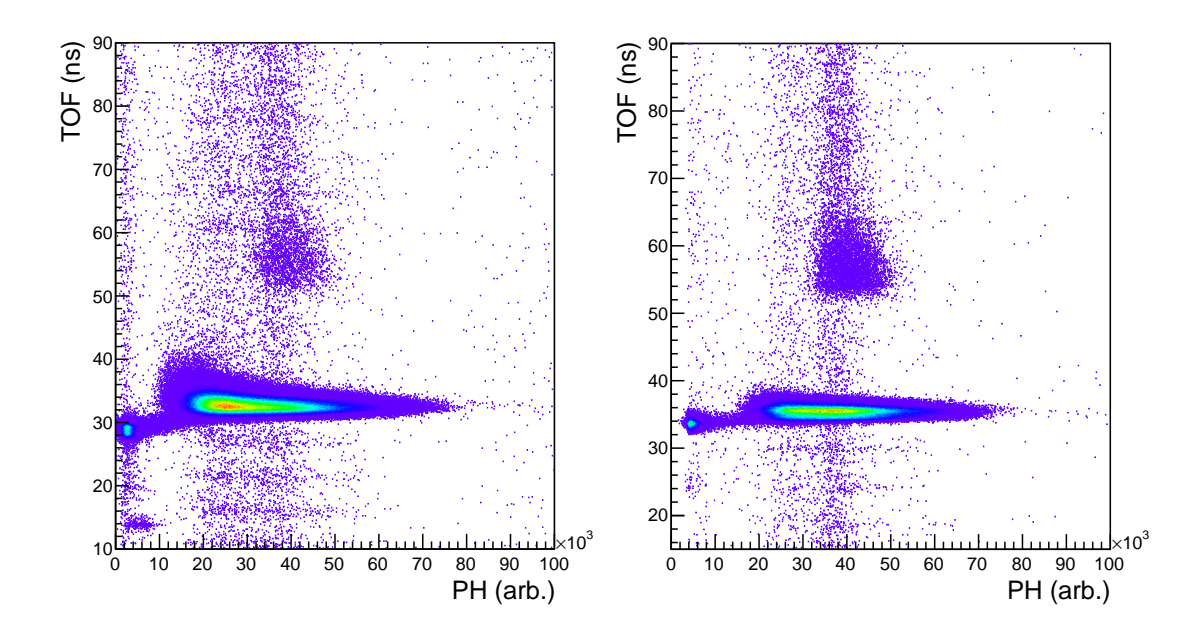


Figure 3. Histograms of TOF vs. PH for the out-of-plane (left) and in-plane detectors (right). The γ -flash can be clearly seen below a TOF of 40 ns and the neutrons are clearly separated above 50 ns.

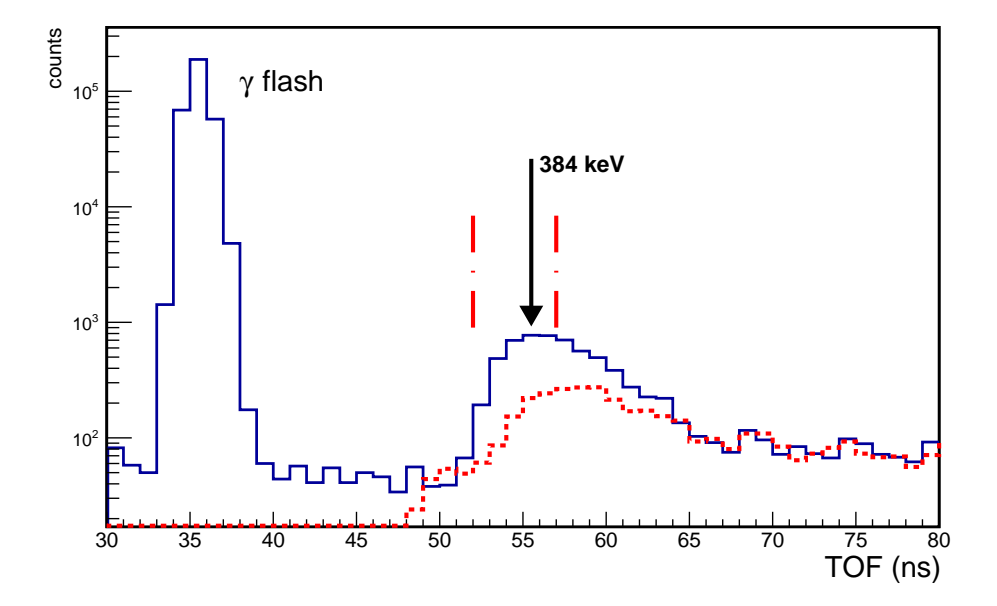


Figure 4. TOF spectrum for the in-plane (solid line) and out-of-plane (dashed line) detectors. The arrow indicates the expected TOF of outgoing neutrons for a mono-energetic gamma beam and thin target. The two dashed red lines indicate the range of the summing window for polarization asymmetry calculation.

trum as this is simpler and avoids the transformation into neutron energy. Nevertheless, an example of the neutron energy spectrum for the in-plane and out-of-plane detectors is shown in figure 5.

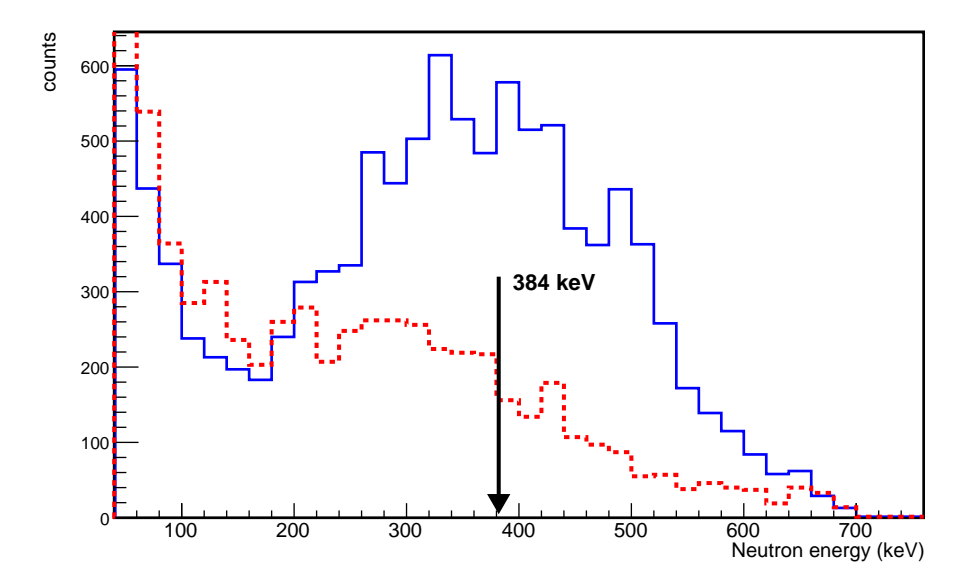


Figure 5. The neutron energy spectra recorded by the in-plane (solid line) and out-of-plane (dashed line) detectors. The arrow indicates the expected 384 keV neutron energy for a mono-energetic gamma beam of 2.997 MeV.

The correction due to finite size was determined by generating neutrons uniformly within the intersection of the target and the beam spot according to the expected angular distribution from ref. [7]. These neutrons then were propagated in the room, and hits were recorded if their paths intersected the detectors. Based on this simple Monte Carlo simulation, we determined that the measured polarization asymmetry should be increased by approximately 3% as a result of finite size corrections.

An analysis was performed to account for the systematic uncertainty in placing the high TOF cut. The polarization asymmetry was determined by varying the position of the high TOF cut, depending on the beam energy while the position of the low TOF cut was kept fixed. The systematic uncertainty was determined by the variation in the polarization asymmetry over this region of cut positions.

Table 3 shows the results of the analysis. The expected asymmetry was determined from the theoretical polarization asymmetries of ref. [7]. The agreement between the measured asymmetry and the expected asymmetry is excellent.

The beam intensity was calculated using Equations 2.3 and 2.4. The summing window for the emitted neutrons was widened to include the entire neutron peak as the lower energy neutrons are still originating from the $d(\gamma,n)p$ reaction. The energy spectrum in figure 5 is folded with the detector efficiency, which was taken from ref. [17]. The calculated intensity for the July 2015 run at 3 MeV is 1.2×10^7 s⁻¹, which is in agreement with the quoted intensity from the control room if we consider that no validation of the neutron detector efficiencies have been performed. Several systematic uncertainties due to the target thickness, detector system, and $d(\gamma,n)p$ cross section are identified for this type of measurement. The most important uncertainties are associated with the detection system: detector efficiency, solid angle, misalignment, and gain drift. We asses that with a well characterized system, the systematic uncertainties can be limited to 3%.

Table 3. Summary of the measurements performed in November 2014 (a) and July 2015 (b) at HI $_{\gamma}$ S at gamma beam energies below 4 MeV. Beam intensities were estimates reported from the control room. (*) The beam polarization is not actually larger than 100%, but can appear to be from the statistical and systematic uncertainties.

E_{γ}	Beam intensity	Time	Expected	Measured	Beam	Uncertainty
(MeV)	$(\times 10^7 \text{ s}^{-1})$	(min)	Asymmetry	Asymmetry	Polarization	Stat. & Syst.
2.50^{a}	1.2	60	0.693	0.688	99.3%	7.3 & 8.2%
2.75^{a}	1.5	60	0.846	0.848	$100.2\%^*$	1.4 & 1.5%
3.00^{a}	1.7	55	0.903	0.903	100.0%	1.8 & 2.6%
3.00^{b}	0.7	78	0.903	0.912	101.0%*	2.5 & 1.3%

4 Measurements at $HI\gamma S$ above 4 MeV

Neutrons from the $d(\gamma,n)p$ reaction at incident gamma-rays above 4 MeV have energies in excess of 800 keV at 90° scattering angles. The neutrons in the energy region around 1 MeV and above are detected with greater efficiency by using NE213-type liquid scintillator detectors. Measurements with BC501 neutron detectors have been carried out at HI γ S during the same experimental campaigns described in section 3. The design and execution of the experiments was conceptually similar to the measurements below 4 MeV.

The BC501 detectors used for measurements above 4 MeV have a liquid scintillator cell of 12 cm diameter and 5 cm thickness, coupled to a Hamamatsu H6527 PMT. Four liquid scintillator detectors have been used to detect the outgoing neutrons during the November 2014 run. Two detectors were placed in the horizontal plane at a scattering angle of 90° (one to the left of the beam and another to the right), and the other two detectors were placed in the vertical plane at a scattering angle of 90° (one above the beam and the other below the beam). The target was composed of heavy water (D₂O) in a 5 cm long and 3.2 cm diameter polyethylene cell. The detectors were placed approximately 71 cm from the target position. The detector signals were sent to Mesytec MPD-4 modules, and the outputs were sent to an ADC and a TDC to record the events.

Measurements were performed in November 2014 at four different energies: 5.0, 7.0, 15.0, and 20.0 MeV. The γ -ray beam generation was different for the present experiments than during the typical operation at HI γ S. During typical HI γ S operations, a set of linear wiggler magnets is used to generate 100% linearly polarized FEL light. However, for these experiments a new method was used to produce nearly 100% linearly polarized FEL light. Therefore, the γ -ray beam linear polarization was no longer consistent with 100%. The results of these measurements are presented in table 4. Several experiments have been performed with this new beam generation method and the d(γ ,n) technique has been successfully used to measure the beam polarization [18].

In July 2015 we have measured the neutrons from $d(\gamma,n)p$ reaction with a 7 MeV incident gamma beam. The gamma-beam has been produced using the OK-4 method which yields beams with linear polarization consistent with 100%. Two BC501 detectors have been used: one detector positioned in the plane of the beam polarization, detector designated as "beam-left detector", and the other positioned perpendicular to the plane of beam polarization (detector designated as "bottom detector"). Both detectors were approximately 76 cm from the center of the target. The BC501

Table 4. Summary of the measurements performed in November 2014 at $HI\gamma S$ at gamma beam energies above 4 MeV. The uncertainties are discussed in the text.

E_{γ}	Expected	Measured	Beam
(MeV)	Asymmetry	Asymmetry	Polarization
5.0	0.959	0.892	93.0%
7.0	0.969	0.907	93.6%
15.0	0.935	0.833	89.1%
20.0	0.898	0.794	88.4%

detectors have the same specifications as those used in November 2014 measurements. The diagram of the setup is shown in figure 2. The detector waveforms were read into a CAEN V1730 14-bit 500 Ms/s digitizer. We describe here the analysis of the data taken in July 2015 with the digitizer although the analysis procedure was identical for the measurements from November 2014.

The analysis steps for these data are well established. The first step is to calibrate the neutron detectors using a gamma-ray source as described in section 2.3. The calibration was used to set a PH threshold at 0.25 of the Compton edge of 137 Cs, or approximately 120 keVee. This threshold eliminates γ rays and neutrons where the pulse shape discrimination (PSD) performance of the detector is not optimal and at the same time allows us to determine a realistic neutron detection efficiency.

The first measurement at each energy was performed using a 100% circularly polarized beam to correct for any differences in detector distance or detection efficiency. We then switched to 100% linearly polarized beams for the asymmetry measurement. The generated pulse shape (PS) versus PH distributions for the in-plane and out-of-plane detectors are shown in figure 6. There is very good separation between gamma-rays and neutrons down to 200 keVee. The PS vs. TOF distributions from figure 7 display also very good separation between photons and neutrons.

We select the neutrons from either PS vs. PH or PS vs. TOF distributions and construct the TOF spectrum. An example of time-of-flight spectra for the in-plane and out-of-plane detectors is shown in figure 8. The arrow line indicates the expected 2.38 MeV energy of the neutrons, corresponding to a TOF channel of 61.5, for a mono-energetic beam of 7 MeV and thin target. The FWHM of the gamma-ray peak in the TOF spectrum is 1.3 ns. The TOF spectrum of the out-of-plane detector has been shifted to align its γ -flash with the in-plane detector.

The measured polarization asymmetry varies depending on the location of the high TOF cut shown in figure 7. The measured polarization asymmetry decreases smoothly as this cut is placed at higher TOF, corresponding to lower neutron energies. There are two causes for this effect: finite size corrections and multiple scattering. These effects arise from using TOF to determine neutron energies. The location of the high TOF cut changes the impact of finite size corrections because it changes the position of the interaction points. Neutrons which were multiply scattered before reaching the detector will appear on the high TOF side of the peak, and they will have a smaller polarization asymmetry than the neutrons which did not multiply scatter.

To account for these effects, a full Monte Carlo simulation of the target and detectors was performed using GEANT4. The simulation code uses the detector distances, sizes, and efficiencies as inputs. It also uses the target dimensions and beam spot size as inputs. Neutrons are generated at the target with the theoretical polarization asymmetries calculated by ref. [7]. The neutron position

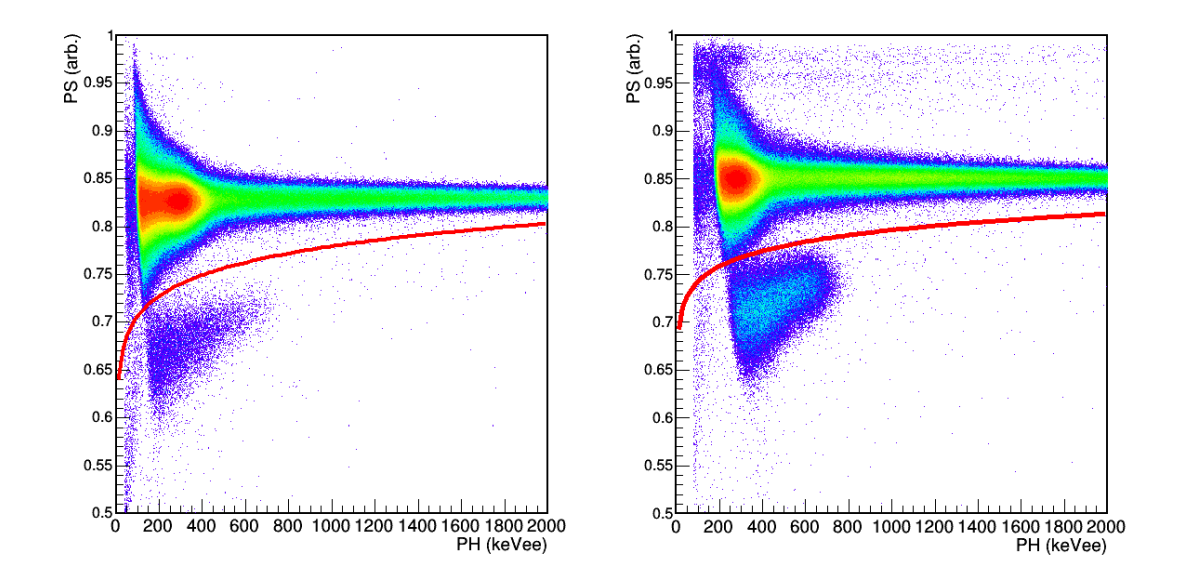


Figure 6. Histograms of PS vs. PH for the out-of-plane (left figure) and in-plain detectors (right figure) with 100% linearly polarized gamma beam. The red line is used to separate neutrons and photons.

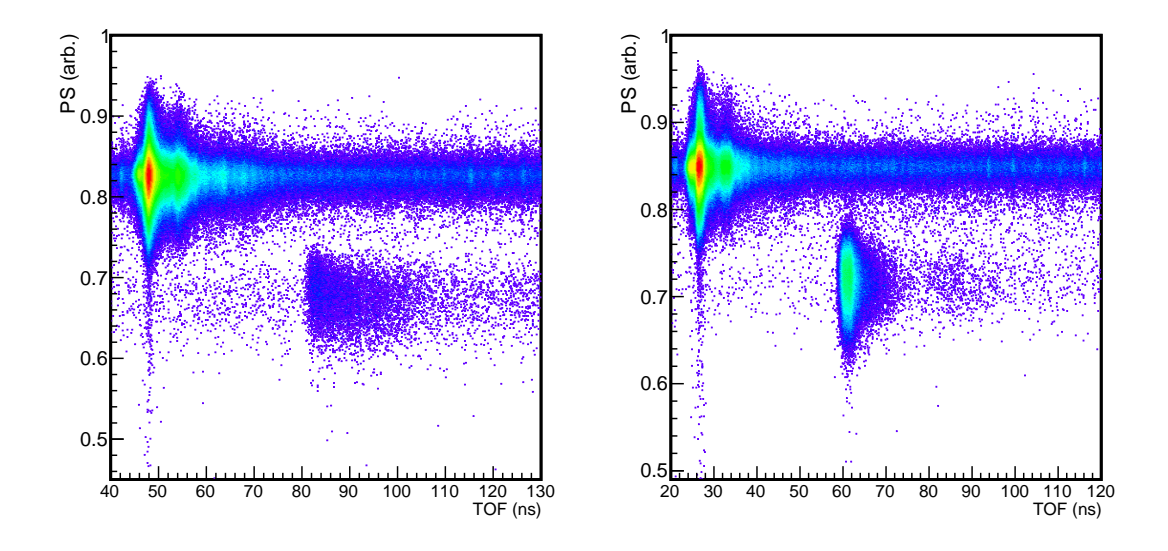


Figure 7. Histograms of PS vs. TOF for the out-of-plane (left figure) and in-plain detectors (right figure) with 100% linearly polarized gamma beam. Neutrons are clearly separated from photons.

is taken at random from within the intersection of the beam spot and the target. These neutrons travel in the simulated experimental hall, and hits are recorded if they interact and deposit sufficient energy in the simulated detectors. The time of each event is recorded relative to the time at which the neutron was generated. The simulated neutron energy spectra are determined from their simulated TOF, just as in the actual measurement. The timing resolution of each detector is adjusted so that the widths of the simulated and measured neutron energy distributions match.

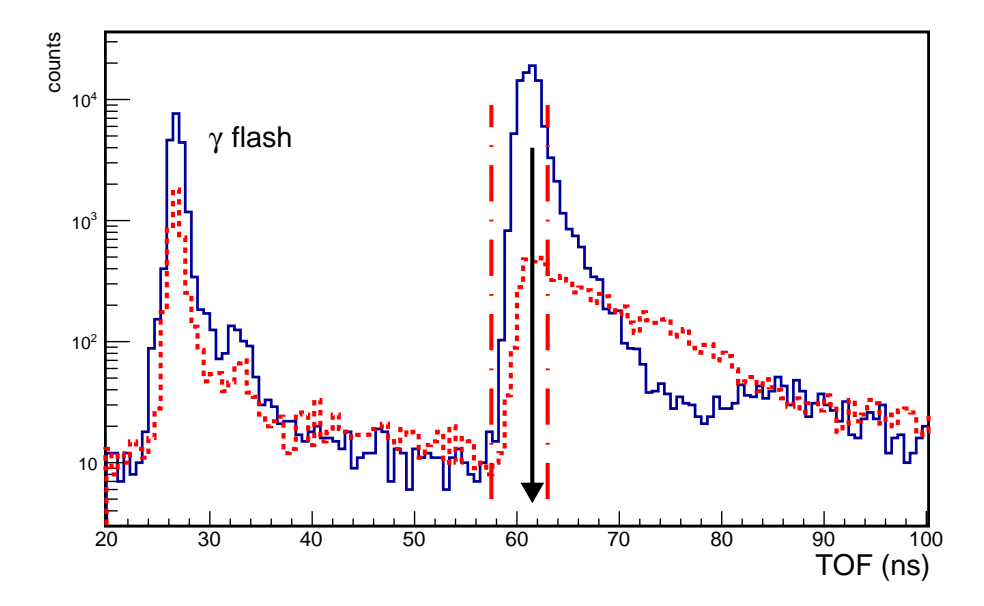


Figure 8. TOF spectrum for the in-plane and out-of-plane (dashed line) detectors for a gamma beam of 7 MeV. The arrow indicates the expected TOF of outgoing neutrons for a mono-energetic gamma beam and thin target. The two dashed red lines indicate the range of the summing window for polarization asymmetry calculation.

Table 5. The result of the measurement performed in July 2015 at $HI\gamma S$ at 7 MeV gamma beam energy.

E_{γ} Expected		Measured	Beam	
(MeV)	Asymmetry	Asymmetry	Polarization	
7.0	0.976	0.978	100.2%	

The result of the measurements performed in July 2015 are presented in table 5.

Several systematic uncertainties were investigated to assess the stability and reliability of this technique. The first systematic uncertainty assessed was the dependence of the extracted beam polarization B_{pol} on the position of the high TOF cut. Apart from statistical fluctuations, B_{pol} is very stable for small changes in the position of the high TOF cut. We assessed this systematic uncertainty to be approximately 0.5%. Other uncertainties include possible small gain shifts in the detectors and slight misalignments of the detectors. Both of these uncertainties are also smaller than 1%. Therefore, the dominant systematic uncertainty is from the uncertainty on the theoretical predictions of ref. [7], which we have taken to be approximately 1%.

The beam intensity was calculated following the procedure described in section 3 by using Equations 2.3 and 2.4. Each energy bin is folded with the detector efficiency at the same energy threshold of 120 keVee or at 0.25 of the Compton edge of 137 Cs. The detector efficiencies were taken from the simulation code used in ref. [19]. The calculated intensity for the July 2015 run at 7 MeV is $3 \times 10^7 \, \mathrm{s}^{-1}$, which is of the same order with the quoted intensity from the control room of between 1 and $5 \times 10^7 \, \mathrm{s}^{-1}$. No precise experimental measurements of the neutron detection efficiency have been performed for the intensity calculations presented in this paper. Thus, the

gamma beam intensity calculations are a proof-of-principle of the method described in section 2.3. The same systematic uncertainties described in section 3 are identified for this type of measurement: target thickness, detector system, and cross section. We asses that with a well characterized system, the overall systematic uncertainty can be limited to below 5%.

5 Conclusion

We have investigated the $d(\gamma,n)p$ reaction for intensity and polarization measurements of the gamma beam at ELI-NP. Based on the measurements at HI γ S we conclude that an instrument based on the $d(\gamma,n)p$ reaction should be constructed for use at ELI-NP. The design of the proposed instrument should consider the temporal structure of the ELI-NP gamma beam. Three ⁶Li-glass detectors of 5-cm diameter and 1-cm thickness and three EJ309-type liquid scintillators of 12-cm diameter and 5 cm-thickness have been already purchased. Full GEANT4 and MCNP simulations of the proposed instrument are underway. A campaign of measurements with mono-energetic neutrons and with a time-tagged ²⁵²Cf ionization chamber to characterize the neutron detectors and to validate the simulations has been approved.

Acknowledgments

CM, GS, and CAU were supported in part by Extreme Light Infrastructure Nuclear Physics (ELI-NP) Phase I, a project co-financed by the European Union through the European Regional Development Fund.

References

- [1] EuroGammaS Association, O. Adriani et al., *Technical Design Report EuroGammaS proposal for the ELI-NP Gamma beam System*, arXiv:1407.3669.
- [2] H.R. Weller et al., Gamma Beam Delivery and Diagnostics, Rom. Rep. Phys. 68 (2016) S447.
- [3] Y. Birenbaum, S. Kahane and R. Moreh, *Absolute cross section for the photodisintegration of deuterium*, *Phys. Rev.* C 32 (1985) 1825.
- [4] R. Bernabei et al., *Deuteron Photodisintegration Total Cross-section Between 15-MeV and 75-MeV*, *Phys. Rev. Lett.* **57** (1986) 1542.
- [5] W. Jaus and W.S. Woolcock, A fit to deuteron photodisintegration data up to 200 MeV using the Nijmegen 1993 potential, Nucl. Phys. A 608 (1996) 399.
- [6] W. Tornow, N.G. Czakon, C.R. Howell, A. Hutcheson, J.H. Kelley, V.N. Litvinenko et al., *Low-energy photodisintegration of the deuteron and big bang nucleosynthesis*, *Phys. Lett.* **B 574** (2003) 8.
- [7] H. Arenhovel and M. Sanzone, *Photodisintegration of the Deuteron: A Review of Theory and Experiment*, Springer-Verlag (1991).
- [8] S. Burles, K. Nollett, J. Truran and S. Turner, *Sharpening the Predictions of Big-Bang Nucleosynthesis*, *Phys. Rev. Lett.* **82** (1999) 4177.
- [9] R. Moreh, T.J. Kennett and W.V. Prestwich, *H-2 (gamma, n) absolute cross section at 2754 keV, Phys. Rev.* **C 39** (1989) 1247 [*Erratum ibid.* **C 40** (1989) 1548-1548].

- [10] J. Ahrens, H.B. Eppler, H. Gimm, M. Kröning, P. Riehn, H. Wäffler et al., *Photodisintegration of the deuteron at 15–25 MeV photon energy*, *Phys. Lett.* **B 52** (1974) 49.
- [11] B.A. Perdue, *Measurements of the Absolute Cross Section of the Three-body Photodisintegration of* 3 *He Between E* = 11.4 MeV and 14.7 MeV at HIGS, Ph.D. thesis, Duke University, 2010 (unpublished).
- [12] G. Dietze and H. Klein, *Gamma-calibration of NE213 scintillation counters*, *Nucl. Instrum. Meth.* **193** (1982) 549.
- [13] C. Matei, F.-J. Hambsch and S. Oberstedt, *Proton light output function and neutron efficiency of a* p-terphenyl detector using a ²⁵²Cf source, Nucl. Instrum. Meth. A **676** (2012) 135.
- [14] R. Nolte and D.J. Thomas, Monoenergetic fast neutron reference fields: I. Neutron production, Metrologia 48 (2011) 263.
- [15] W. Mannhart, Evaluation of the Cf-252 fission neutron spectrum between 0 MeV and 20 MeV, in Proceedings of an Advisory Group Meeting on Properties of Neutron Sources, Leningrad, USSR, 9–13 June 1986, IAEA-TECDOC-410 IAEA, Vienna, (1987) 158.
- [16] Y. Wu, V.N. Litvinenko, B. Burnham, J.M.J. Madey and S.H. Park, *The performance of the Duke FEL storage ring*, *Nucl. Instrum. Meth.* A 375 (1996) 74.
- [17] V.N. Kononov et al., Neutron detection efficiency of a thick lithium glass detector, Nucl. Instrum. Meth. A 234 (1985) 361.
- [18] J.M. Mueller et al., Tests of a novel method to assay SNM using polarized photofission and its sensitivity in the presence of shielding, Nucl. Instrum. Meth. A 776 (2015) 107.
- [19] D.E. Gonzalez Trotter et al. Neutron detection efficiency determinations for the TUNL neutron-neutron and neutron-proton scattering-length measurements, Nucl. Instrum. Meth. A 599 (2009) 234.